論文 / 著書情報
Article / Book Information

Title	Mobilisation of earth pressure acting on pile caps under cyclic loading
Authors	Akihiro Takahashi, Hideki Sugita, Shunsuke Tanimoto
Citation	Soils and Foundations, Vol. 48, No. 6, pp. 741-754
Pub. date	2008, 12

Mobilisation of earth pressure acting on pile caps under cyclic loading

by Akihiro Takahashi, Hideki Sugita and Shunsuke Tanimoto

Abstract

In lateral resistance of piles with a pile cap, marked contribution of the pile cap resistance can be expected. For seismic performance assessment of pile foundations, mobilisation of the earth pressure acting on pile caps, induced by interactions between the pile cap and surrounding soils, has to be properly considered. In this study, a series of centrifuge model tests were conducted (1) to examine the effect of strain history on the mobilization of lateral earth pressure acting on pile caps and (2) to show the importance of considering strain history when modelling the interaction between a surface soil layer and a pile cap. Observations in the physical model tests reveal that mobilisation of the earth pressure acting on pile caps under cyclic loading can drastically change depending on soil type and/or conditions. Especially, relocation of soil adjacent to the pile cap in unload—reload phase plays an important role for the earth pressure mobilisation, as it completely alters the shape of the earth pressure—displacement curves. Based on the physical model test results, a simple empirical model that can be used for the beam on non-linear Winkler foundation type analysis is proposed and compared to the test results.

Keywords: centrifuge model test, cyclic loading, passive earth pressure, pile cap, sand (E08/E12/G14)

Soils and foundations 48 (6), 741-754, 2008

Original URL:

http://dx.doi.org/10.3208/sandf.48.741

INTRODUCTION

In lateral resistance of piles with a pile cap, marked contribution of the pile cap resistance can be expected. Recent lateral load tests on full scale piles with a pile cap (Mokwa & Duncan 2001, Rollins & Sparks 2002, Rollins & Cole 2006, among others) reveal that the pile cap provides large portion (30—50% in the cited papers) of the overall resistance of the pile groups to lateral loads. Apart from the positive side mentioned above, a pile foundation is vulnerable from the lateral force acting on the pile cap when the foundation soils are susceptible to laterally spread due to liquefaction. Piles have been severely damaged in past earthquakes by a non-liquefied surface layer spreading laterally over an underlying liquefied soil layer and the load induced by the interaction of this surface "crust" with the structure is believed to dominate the response of pile foundations subjected to these conditions (e.g., Berrill & Yasuda 2002, Finn & Fujita 2005, Takahashi et al., 2006, Brandenberg et al. 2007). In any case, mobilisation of the earth pressure acting on pile caps induced by interactions between the pile cap and surrounding soils has to be properly considered in pile foundation performance assessments.

To examine required displacements for mobilisation of the full passive earth pressure under various wall movements, many physical model tests have been undertaken. (Most of the tests were on relatively small models.) Rowe & Peaker (1965) and James & Bransby (1970) examined the passive earth pressures acting on a rotational wall and compared them with the theoretical values. Narain et al. (1969) measured the displacement required to cause maximum pressures when three types of the wall displacement are given, i.e., translation and rotation about the bottom and top. The similar tests were also performed by Fang et al. (1994 & 1997). Rollins & Sparks (2002) reviewed several passive pressure load tests in the past and showed that the displacements required to reach the full passive pressure were in a range of 2.5—6% of the wall height.

Recently lateral load tests on full scale piles with a pile cap were undertaken (e.g., Mokwa & Duncan 2001, Rollins & Sparks 2002) and indirectly showed how the earth pressure acting on the pile cap was mobilised in the monotonic loading. Duncan & Mokwa (2001) performed monotonic passive pressure load tests in intact natural ground and compacted backfill with gravel and compared them with the values obtained from the log spiral theory and the hyperbolic load—displacement curve.

Generally the previous tests mentioned above focused on the passive pressures in the monotonic loading.

For cyclic loading, Rollins & Cole (2006) and Cole & Rollins (2006) reported changes of the earth pressure acting on a pile cap, based on a series of the cyclic loading tests on piles with the pile cap and used four different backfill materials from the fine sand to coarse gravel. In the tests, they applied “one-way” loading. As the backfill materials used were moist soils and no active failure of the ground adjacent to the pile cap may have occurred in unload phase, the earth pressure—displacement curves in reload phase retraced the unload curves for all the cases. However, if such an active failure occurs in unload phase, shape of the reloading curve may change and the reloading curve may not coincide with the unload curve.

In this study, a series of centrifuge model tests were conducted to examine the effect of strain history on the mobilization of lateral earth pressure acting on pile caps. This paper shows the importance of considering strain history when modelling the interaction between a surface soil layer and a pile cap. In data analysis, special attention is paid to relocation of soil adjacent to the pile cap in unload—reload phase, as it may completely alter the shape of the earth pressure—displacement curves. Based on the physical model test results, a simple empirical model that can be used for the beam on non-linear Winkler foundation type analysis is proposed and compared to the test results.

OUTLINE OF PHYSICAL MODEL TESTS

Model setup

Because the focus of this study was the examination of lateral earth pressure acting on pile, a pile cap only —without piles— was modelled. Figure 1 shows a diagram of the centrifuge model package. In a real foundation, the earth pressure acting on a pile cap is the result of the interaction between the moving surface soil layer and foundation. However, because this is difficult to simulate in a centrifuge while controlling the relative displacement between the pile cap and the surrounding soil, the relative displacement was created by horizontally displacing a model pile cap in motionless model ground, using an electric actuator. In the tests, the model surface layer was relatively thick as shown in Fig. 1, neglecting the existence of the soft soil layer underneath the surface layer. As (1) Rollins & Sparks (2002) pointed out that a weak soil layer under the surface layer could make the required displacement to mobilise the full passive pressure larger and (2) Brandenberg et al. (2007)

demonstrated such effects using simple load transfer models, the obtained displacement to mobilise the passive earth pressure in this study could be smaller than the cases with a weak soil layer just below pile caps.

A front view of the model pile cap is illustrated in the lower left of Fig. 1. Two 2-directional load cells were placed on the front face of the pile cap to measure the normal and shear stresses acting on the centre and edge of the cap. In order to minimize friction between the pile cap and the surrounding ground at the top, bottom and sides, 0.3mm-thick latex membranes were attached to those faces with grease. Particles of Toyoura sand were glued to the front face, to roughen that surface. The heave of the ground surface in the proximity of the cap at DV3 was measured by a LVDT fixed on the centrifuge model container.

Load tests were performed at 50g by changing the geomaterial, the depth of the pile cap (D), and the loading pattern, as shown in Table 1. A typical road bridge foundation in Japan has pile caps about 8m wide and 2m thick when it has three cast-in-place concrete piles in a row. According to scaling laws for the geotechnical centrifuge modelling, the model pile cap should be 1/50 of that size when the tests are conducted at 50g. However, due to the limited capacity of the electric actuator used, the tests were performed on a 1/100 model at 50g.

Materials used

In the tests, two sands were used. One was Toyoura sand and the other was Edosaki sand. The former was used under dry condition, while the latter was used for modelling moist sand. For the tests using Toyoura sand, specimens were prepared by the air-pluviation method, using air-dried sand. For the tests using Edosaki sand, specimens with near-optimum water content of 15% were compacted in layers to a dry density of 1.49Mg/m^3 (bulk density $\rho_t = 1.72$Mg/m^3) on the laboratory floor, corresponding to a relative compaction of 90%. The maximum density (the reference density for the relative compaction) and the optimum water content were determined according to the standard test method for soil compaction using a rammer (JIS A 1210: 1999, Method A-b, which is equivalent to ASTM D698-07e1, Method A.) Although the specimens were compacted with water content of 15%, drainage induced during centrifugal acceleration of the model ground to 50g resulted in final estimated average water content of about 10% ($\rho_t \approx 1.65$Mg/m^3.) To obtain the strength parameters for the material used and the frictional characteristics of the interface between the soils and front face of the pile cap, the direct shear tests were performed. The test results are summarised in Table 2.

Test conditions

Two cyclic loading conditions were adopted in this study: (1) One is to gradually increase horizontal relative displacement between the surface layer and pile cap during cyclic loading, and (2) "two-way" cyclic loading followed by the monotonic loading. The former may correspond to a soil—abutment interaction (as seen in Takahashi et al., 2007) or soil—pile foundation interaction in the laterally spreading soil during earthquake. These impose different strain histories on the surface soils, along with a potential for differences in the mobilization of lateral earth pressure acting against a pile cap. To investigate these types of strain history effects on lateral earth pressure mobilization, three loading patterns were employed, as shown in Table 1. "Cyclic1" corresponds to the first loading pattern described above, while "Cyclic2" is the second. In addition to these two patterns, monotonic loading was also conducted. Typical loading patterns are illustrated in Fig. 2. The tests were performed "statically" in order to remove potential inertia forces; a very slow loading rate (3mm/min) was employed in all the loading cases.

MOBILISATION OF PASSIVE EARTH PRESSURE

Dry Toyoura sand under cyclic loading

Figure 3 shows how the mobilized earth pressure coefficient, $K = \sigma_h / \sigma_v$, varies with the pile cap horizontal displacement (u) normalised by the pile cap height (H), u/H, for the dry Toyoura sand cases, where σ_h =horizontal stress and σ_v =vertical stress. The mobilized earth pressure coefficient was calculated from (1) the average horizontal stress acting on the pile cap, which was measured at L1 and L2, and (2) the initial vertical stress at the mid-height of the pile cap. It should be notice here that, with the earth pressure coefficient defined above, the calculated passive earth pressure coefficient based on this definition can be much larger than those obtained from the classical plasticity theory or the soil element tests, as the change of the vertical stress at the mid-height of the pile cap due to the ground surface heaving is not taken into account. The displacement required to reach the first peak is smallest for the Cyclic2 loading pattern, largest for the Monotonic loading, and intermediate for Cyclic1. Even though the graph in Fig. 3 is crowded with data points in the small displacement region, this behaviour can be seen for both of the pile cap embedment depths (*D*) that were tested. This indicates that sand which has undergone many strain cycles before reaching a first peak in mobilized earth pressure will reach that first peak after a smaller pile cap displacement than a sand that has been subject to a small number of strain cycles (cf. subsequent Fig. 4.) The results also show, as expected, that increasing the pile cap embedment depth will increase the amount of horizontal pile cap displacement necessary to reach the first earth pressure peak.

These results are related to the relocation of soil adjacent to the pile cap that occurs when the cap moves away from the soil during the unload phase of unload—reload cycle. Backward movement ($\Delta u < 0$) of the cap creates an active state in the soil adjacent to the cap, as shown by a rapid drop in the earth pressure. This allows the soil adjacent to the cap to move downward, filling a gap that has formed between the cap and the surrounding soil, i.e., the local active failure of the ground occurs during this process. Successive reloading ($\Delta u > 0$) acts to compact the in-filled sand and pushes it forward. Particularly near the bottom of the pile cap, as the gap is fully filled with sand as long as the enough sand supply from the top exists, this compaction hardens and pushes further the soil in front of the pile cap and imposes higher strains in the soil distant from the cap than would be likely to occur without such cycles. Therefore, a pile cap that has experienced cyclic displacement relative to the surrounding soil requires a smaller pile cap displacement to cause general shear failure of the soil in front of the cap. This phenomenon is know as "racheting effect" and has been recognised in the earth pressure change acting on integral bridge abutment due to the soil-structure interaction (e.g., Ng *et al*. 1998). However, the Edosaki sand cases showed different soil responses, as discussed in the following subsection.

Changes of the normal and shear stresses acting on the pile cap, τ , against the normalised horizontal displacement for the Toyoura sand with $D/H = 2$ are shown in Fig. 4, together with the changes of the heave of the ground surface in the proximity of the cap at DV3, v_3 (see Fig. 1.) All the plots are only for the small displacement region and the stresses were measured at the pile cap centre (L2.) Downward shear stress acting on the pile cap is taken as positive. As seen in the figure, the shear stress starts decreasing as soon as the loading direction is changed from unloading to reloading. This fact indicates that the cap was in contact with the soil at the end of unload phase, i.e., the soil adjacent to the cap moved downward and filled a gap that has formed between the cap and the surrounding soil when unloaded. Thus, the shear stress response as well as normal stress (earth pressure) response confirm the filling a gap process in unload—reload cycle.

By coming back to Fig. 3, it can be also noticed that pushing the pile cap beyond the first peak in earth pressure resulted in large geometrical changes to the ground surface, and the earth pressure vs displacement curves become more complicated. In every case except for monotonic loading with $D/H = 2$, the first peak is followed by several more peaks, e.g., local maximal points can be seen at $u/H = 6$, 36, 75% for Cyclic1 with $D/H = 1$. (If more displacement is imposed in the case with $D/H = 2$, several peaks could be observed for this case as well.) The interval between peaks depends upon the loading history and the embedment depth of the pile cap, as follows: (1) the larger the number of loading cycles, i.e., Cycle2, Cycle1 and Monotonic, in descending order, the shorter the interval between peaks, and (2) the larger the pile cap embedment depth, the longer the interval between peaks. Visual observation of the ground surface during the tests revealed that the drop in the earth pressure coincided with the appearance of the edge of a slip plane on the ground surface (a shear zone); outer slip surfaces, further from the pile cap, were observed during subsequent drops in the earth pressure. In brief, the large displacement of the pile cap greatly changes the geometry of the ground surface and hence causes many local maximal points in the earth pressure vs displacement curves depending on the strain history. In many cases, implementation of this feature may not be relevant in design practice. However, in the cases where the large relative displacement between the pile cap and surrounding ground is expected, e.g., a pile foundation in the lateral spreading of liquefiable soils, consideration of this fluctuation of the passive earth pressure or determination of a representative value for the upper limit of the earth pressure can be a crucial factor.

Apart from the geometrical change of the ground surface in a large sense, the process of the local active failure and pressing of the soil adjacent to the pile cap in the cyclic loading can make larger the strain imposed to the soil distant from the cap, resulting in a smaller displacement to cause general shear failure of the soil in front of the cap. Not only the timing of the passive earth pressure mobilisation, but also the relationship between the earth pressure and pile cap displacement during cyclic loading before reaching the passive state are affected by the response of the soil adjacent to the pile cap. One of examples for the latter is shown in Fig. 5: Figure 5 plots time histories of the normal stress measured at L2 and normalised imposed displacement for Cyclic2 with $D/H = 2$. The maximum earth pressure mobilised increases with each successive loading cycle in a loading phase when the maximum pressure is below the passive earth pressure. For instance, in Phase 2 the maximum earth pressure mobilised increases with each cycle, while it keeps more or less constant value in Phase 3 since the maximum pressure for each cycle has reached the passive earth pressure. Although the degradation due to the cyclic loading is reported in the published papers for piles and pile caps (Shirato et al. 2006, Rollins & Cole 2006, among others) the increase of the maximum earth pressure mobilised with each successive loading cycle does not seem to emphasis in the previous works. Analysis results of these aspects including the example mentioned above are described in detail through response comparisons between the dry and moist sands, subsequently.

Moist Edosaki sand under cyclic loading

In this subsection, the effect of strain history on the mobilization of lateral earth pressure in Edosaki sand is examined and compared to the effect strain history had on dry clean Toyoura sand. The Edosaki sand tests were designed to model more realistic conditions, in which the surface soil may be partially saturated, and is likely to contain fines. With these conditions, the backfill may be self-supportable and the gapping between the pile cap and backfill can be expected during cyclic loading. Tokimatsu (2003) performed a series of large-scale shake table tests on a pile foundation in horizontally layered sand with fines ($F_C = 5.4$%) and observed gap between the pile cap and backfill during shaking. Rollins and Cole (2006) conducted a series of the cyclic loading tests on piles with a pile cap and used four different backfill materials from the fine sand to coarse gravel. They reported that the gap between the pile cap and backfill appeared during the one-way cyclic loadings and got larger with increase of the input displacement magnitude. The test results reveal that the mechanism causing changes in the earth pressure mobilization in Edosaki sand with apparent cohesion is different from the mechanism at work in the dry Toyoura sand tests but is similar to the large-scale tests mentioned above. Details of the Edosaki sand tests are described below.

The earth pressure vs normalised pile cap displacement curves for the Edosaki sand are shown in Fig. 6, together with the changes of the heave of the ground surface in the proximity of the cap at DV3. For $D/H = 2$, changes of the shear stress acting on the pile cap are also plotted. All the stresses in the figure were measured at L2. When $D/H = 1$, pre-peak strains in the Edosaki sand have an effect similar to the effect seen in the Toyoura sand: a certain number of strain cycles before the first peak in mobilized earth pressure results in a smaller required displacement to reach that peak, although no large difference can be seen in the earth pressure vs displacement curves between Cyclic1 and Cyclic2. On the other hand, when $D/H = 2$, this effect is not seen, at least not in the small displacement region where $u/H < 20\%$ and the envelopes of the curve are approximately identical, irrespective of the loading pattern.

Before describing observations for the Edosaki sand cases in detail, the following fact should be noted: In the cases where $D/H = 1$, i.e., the no covering soil existed above the top surface of the pile cap, excessive evaporation occurred and it may have led to drying and desiccation of the soil surface exposed to the air at the gap between the pile cap and adjacent soil as well as the ground surface in Cyclic1 and Cyclic2, due to the spinning of the centrifuge. This desiccation reduced the water content of the soil adjacent to the pile cap and probably made the adjacent soil stiffer and stronger during the course of the cyclic loading, resulting in the large passive earth pressure in Cyclic1 and Cyclic2, while such large difference was not observed in the cases where $D/H = 2$ since the gap between the pile cap and adjacent soil was not exposed and the drying and desiccation of the soil surface little affected on the passive resistance. If the desiccation did not occur in the $D/H = 1$ cases, perhaps the envelopes of the curve for Cyclic1 and Cyclic2 might be comparable to Monotonic. Due to this fact, hereafter detailed comparisons of the soil responses between monotonically and cyclically loaded soils for the Edosaki sand cases where $D/H = 1$ will not be made.

In the Edosaki sand cases, irrespective to the embedment depth of the pile cap, the reload curve retraces the unload curve before u/H becomes about 10%, suggesting that "refilling" of the soil did not occur during unload—reload cycles probably due to the apparent cohesion, at least, before reaching the passive earth pressure. On the other hand, once the mobilised earth pressure reaches the passive state, the gap seems to be partially closed by the soil during unload phase in the larger displacement region ($u/H > 20\%$) for the cases where $D/H = 2$. The former "no-refilling" of the soil during unload—reload cycles is explained in detail using Fig. 7: Figure 7 plots time histories of the normal stress measured at L2, normalised maximum pile cap displacement experienced and normalised imposed displacement for Cyclic2 with $D/H = 2$. The earth pressure vs normalised displacement curves in Phases 3 and 6 are also plotted in the figure. (Phase 6 is the monotonic loading that follows the cyclic loading.) In Phases 1 and 2, as the maximum displacement imposed in each loading cycle in a loading phase is the maximum value up to that stage, in the second and third cycles in a loading phase the state point in the earth pressure vs displacement plane retraces the unloading curve in the first cycle and mobilises a certain amount of earth pressure at the maximum displacement point. Unlike Toyoura sand cases, the some degradation occurs in the second and third cycles in a loading phase. In the third cycle of the Phase 3 and the following loading cycles in Phases 4 and 5, since the maximum displacement imposed in each loading cycle in a loading phase is smaller than the maximum value experienced, the state point in the earth pressure vs displacement plane traces the unloading curve in the second cycle of the Phase 3 and does not show any increase in the earth pressure. These indicate that the widened gap in the successive cyclic loading hardly close with the cyclic loading with the smaller displacement amplitude and requires the displacement comparable to or greater than the maximum value experienced to mobilise the earth pressure. Perhaps in an earthquake the ground shaking, which is not modelled in this study, may help the adjacent soil close the gap. Even so, still a soil similar to the Edosaki sand, e.g., moist pit run sand with fines, may require the more displacement than seen in the dry Toyoura sand tests.

Due to the “no-refilling” of the soil during unload—reload cycles, the heaving near the cap as well as the envelopes of the earth pressure vs displacement curve are approximately identical for $D/H = 2$, irrespective of the loading pattern in the small displacement region. The small and similar heave of the ground surface in the proximity of the cap during that stage suggests that pile cap displacement contributes to quite limited localised deformation of the soil adjacent to the cap, but does not have a large effect on strains in the soil distant from the cap. The former may be attributed to the soil arching or similar effect that creates a roof over the gap and limits the amount of in-filling sand. As a result of these, no marked difference can be seen in the envelopes of the curve.

EARTH PRESSURE CHANGE IN UNLOAD—RELOAD CYCLES

Observations in the physical model tests reveal that mobilisation of the earth pressure acting on pile caps under cyclic loading can drastically change depending on soil type and/or conditions. To model the mobilisation of the earth pressure acting on pile caps under cyclic loading, the followings have to be established; (1) the soil stiffness change in unload—reload phase and (2) the timing of the passive earth pressure mobilisation under cyclic loading. In this section, as the gap opening and closing in unload—reload cycles affect the both two aspects mentioned above, first, these are described in detail to show (1) width of the apparent gap formed in the unload phase and (2) how to define the backbone curve for the earth pressure—displacement relation. The latter is used not only to describe the general shape of the earth pressure—displacement relation but also to determine the timing of the passive earth pressure mobilisation under cyclic loading. Finally, based on the gap formation mechanism, the soil stiffness both in unload and reload phases are modelled.

Gap opening and closing

Width of the gap between the pile cap and adjacent soil varies with the loading history. To quantify the gap width, two parameters are introduced. Figure 8 shows one of the loading cycles in the relationship between the earth pressure and pile cap horizontal displacement. The soil is unloaded from Points A to C through Point B, and then it is reloaded from Points C to E through Point D. From Points A to B, even though an irregular movement of the state point can be seen in the figure, the soil is more or less elastically unloaded. Around Point B, the adjacent soil approaches the active state. From Points B to C, i.e., when the cap move away from the soil, all or part of the formed gap is closed. The soil behaviour in reload phase (from Points C to E) depends on what happened in the phase from Points B to C: In the case where the gap is fully filled with sand when unloaded, as the cap contacts the adjacent soil from the beginning, Point D is almost identical to Point C, and the earth pressure increases to Point E when reloaded. On the other hand, in the case where the gap is not closed when unloaded, Point D is almost identical to Point B and the state point retraces the unloading curve when reloaded. To define Point D, two parameters, δ_G and δ_F, are introduced as shown in the figure. δ_G is an apparent gap between the cap and adjacent soil when unloaded and no resistance is expected in this region when reloaded. This corresponds to the distance between Points C and D in the figure. δ_F is an index that represents amount of soil that pins in the gap during unload phase and corresponds to the distance between Points B and D in the figure. Hereafter δ_F is referred to as “infilling soil index.” When the gap is fully in-filled during unload phase, $\delta_G = 0$, while $\delta_F = 0$ when no closure of the gap occurs during unload phase.

Changes of the apparent gap, δ_G, with the pile cap displacement after the adjacent soil reaching the active state in unload phase, $\delta_F + \delta_G$, are shown in Fig. 9 for all the cases. In the cases with the Cyclic2 loading pattern, $\delta_F \approx 0$ for Edosaki sand, while δ_G increases with $\delta_F + \delta_G$ up to around 0.5mm and levels off for Toyoura sand. The former indicates that the reload curve retraces the unload curve as mentioned in the previous section. For the latter, it can be said that most of the gap is closed by the in-filling sand, i.e., $\delta_G \approx 0$, although the small apparent gap still exists. Probably this small apparent gap is not a real gap but is attributed to the relatively larger compressibility of the in-filling sand.

In the cases with the Cyclic1 loading pattern that imposed very large pile cap displacement during cyclic loading, the apparent gap is very small even for Edosaki sand, while the apparent gap formed in the Edosaki sand cases in Phase 1 show similar response as seen in the cases with the Cyclic2 loading pattern, i.e., $\delta_F \approx 0$. (Even though the Edosaki sand test with $D/H = 1$ shows larger δ_G in Phase 2, attention should not be given to this, since it may be related to the drying and desiccation of the soil surface as mentioned in the previous section.)

Figure 10 plots time histories of the heave of the ground surface in proximity to the cap at DV3 and pile cap horizontal displacement. In Phase 2 where the large pile cap horizontal displacement was imposed, large heave of the ground surface occurred. In the Toyoura sand case where $D/H = 1$, the ground surface slightly subsides and shows plateau in the plot after the adjacent soil reaching active state in unload phase. On the other hand, in the cases where $D/H = 2$, especially in the Edosaki sand case, there is no plateau seen in the Toyoura sand case where $D/H = 1$ and the subsidence continues even after the achievement of active state in unload phase. The latter indicates that the soil distant from the pile cap was continuously deformed during unload phase and may have contributed to close the gap. As this is not pronounced in the cases with the Cyclic2 loading pattern, this may be related to instability of the distant soil due to the surcharge above the pile cap top as well as the geometrical change of the ground surface.

In short, $\delta_G \approx 0$ for the dry sand (Toyoura sand), while $\delta_F \approx 0$ for the moist sand (Edosaki sand) as long as the pile cap horizontal displacement is not large. However, if the large displacement is concerned, $\delta_F > 0$ even for the moist sand.

Backbone curve

In the Edosaki sand cases, the envelopes of the earth pressure vs pile cap displacement curve are approximately identical for $D/H = 2$, irrespective of the loading pattern, i.e., the monotonic loading curve can be used for defining the envelope of the curves for the various loading patterns and can be said to be a backbone curve. On the contrary, at first glance, the monotonic loading curve cannot be a backbone curve for Toyoura sand, since the state point in the earth pressure—pile cap displacement plane moves around outside the monotonic loading curve and the point movement appears to be independent from it, especially for Cyclic2 (cf. Fig. 3.) These indicate that the pile cap displacement is not necessarily a representative value for describing the state point movement in the earth pressure—displacement plane in reference to the backbone curve, especially for Toyoura sand.

Figure 11 is a schematic diagram showing the required soil particle displacement to reach the passive earth pressure at various locations in the ground. Due to the progressive nature of the shear band formation in a compressible material, the displacement of a soil particle, at the time the earth pressure acting on the pile cap reaches the passive state, varies according to the particle's location. The displacement of the soil particle adjacent to the pile cap, e.g., at Point R_A in the figure, may depend on the loading history. However, at the points relatively distant from the pile cap, e.g., Points R_B, R_C & R_D in the figure, the required displacement to reach the passive earth pressure may not be affected by the loading pattern very much and may be comparable to that in the monotonic loading. If Point R_B is (1) not far from the pile cap, (2) located above the general shear failure surface formed when the full passive earth pressure is mobilised, and (3) free from the local active failure induced by cyclic loading, irrespective of the loading pattern, the displacement required to reach the passive at Point R_B is almost the same as that of the pile cap in the monotonic loading.

Figure 12 is a schematic diagram showing the deformation of sands adjacent to pile caps in unload—reload cycle. The first column corresponds to the state at Point A in Fig. 8 and the second and third columns are for Points C and E, respectively. The reference particle indicated by the open circle in the figure is a particle that satisfies the above mentioned conditions for Point R_B in Fig. 11. For moist sand, although it is not relevant to the reference particle movement, two apparent gap opening mechanisms can be assumed as shown in the figure. Since the normal stress acting on the pile cap did not reach zero when unloaded and the shear stress was positive and kept more or less constant value at the beginning of reload phase (see Fig. 6,) the mechanism at work in the Edosaki sand tests was that shown in the bottom of the figure.

The point that needs to be emphasised here using Fig. 12 is how the reference particle moves depending on the soil type in unload—reload cycle. For the dry sand (Toyoura sand,) the gap formed between the pile cap and adjacent soil is filled with sand when unloaded. And then, the pile cap moves back to the reference position with pushing the soil in front of the cap in reload phase. In this phase, as $\delta_G \approx 0$, the reference particle moves forward by magnitude of displacement comparable to δ_F, provided compressibility of the in-filled soil is not large. On the other hand, for the moist sand (Edosaki sand,) as $\delta_F \approx 0$, the reference particle does not move in this unload—reload cycle.

Based on the mechanism mentioned above, here a new displacement parameter, the displacement of the reference particle in Fig. 12, is introduced to formulate the earth pressure—displacement relation under cyclic loading. This reference particle displacement, u_R, can be expressed as follow:

$$u_R(t) = u(t) + \alpha \int_0^t \left(-\frac{u(t)}{|u(t)|} \dot{\delta}_F(\tau) \right) d\tau = f_R(u, \dot{\delta}_F, t), \qquad (1)$$

where $u(t) =$ pile cap displacement at time t, $\alpha =$ adjustment parameter. As δ_F is a distance between Points B and D as shown in Fig. 8, $\delta_F(t) \geq 0$ and $\dot{\delta}_F(t) \geq 0$. If the compressibility of the in-filled sand is not large and the reference particle is proximity to the pile cap, $\alpha \approx 1$. If not, $0 \leq \alpha < 1$. The equation intends to feature the fact that u_R does not change when the pile cap moves away from the backfill without gapping, i.e., (1) $\dot{u}_R \approx 0$ when $|\dot{u}| \approx \dot{\delta}_F > 0$ (if $\alpha = 1$) and (2) $\dot{u}_R = \dot{u}$ elsewhere. The state point represented by this index (u_R) and the earth pressure acting on the pile cap, (u_R, σ_h), is the projection point of (u, σ_h) on the earh pressure—pile cap displacement plane for the monotonic loading curve.

As shown in the previous section, for the Edosaki sand tests with $D/H = 2$, as $\delta_F \approx 0$ when the pile cap displacement is not large ($u/H < 20\%$), $u_R \approx u$ and the monotonic loading curve envelops the earth pressure vs reference particle displacement curve for Cyclic1 and Cyclic2. For all the Toyoura sand tests, the mobilised earth pressure coefficient, $K = \sigma_h / \sigma_v$, against the normalised displacement of the reference particle in the backfill, u_R / H, is plotted in Fig. 13, supposing $\alpha \approx 1$. This plot is similar to Fig. 3, but the pile cap displacement, u, is replaced by the reference particle displacement, u_R. By changing u into u_R, the monotonic loading curves ($u_R = u$) envelop the earth pressure—displacement curves for the cyclic loading cases. For $D/H = 2$, the monotonic loading curve satisfactorily envelops the cyclic loading curves, while the cyclic loading curves are located below the monotonic loading curve for $D/H = 1$. For the latter, as there was no covering soil above the pile cap top, the amount of sand that filled the formed gap when unloaded was limited, resulting in the subsidence of the ground surface just in front of the pile cap. This may have led to the smaller passive earth pressure for the cyclic loading cases with $D/H = 1$, compared to the monotonic loading. In addition to this, in the cases with $D/H = 1$, the required reference particle displacement to reach the local maximal points following the first peak for the cyclic loading cases seems to get closer to that for the monotonic loading. This fact supports assumptions that (1) the displacement of the reference particle introduced is comparable to that of the pile cap in the monotonic loading and (2) for the soil particles located relatively distant from the pile cap, the required displacement to reach the passive earth pressure is not affected by the loading pattern very much and is comparable to that in the monotonic loading, as explained using Fig. 11.

In summary, when the earth pressure change in the cyclic loading is plotted against the reference particle displacement in backfill, the monotonic loading curves envelop the cyclic loading curves and can be used as the backbone curve. The reference particle is a particle that is (1) not far from the pile cap, (2) located above the general shear failure surface formed when the full passive earth pressure is mobilised, and (3) free from the local active failure induced by cyclic loading.

Soil stiffness change in unload—reload phase

Provided the backbone curve from the monotonic loading test and the information mentioned above, remaining parts required to model the earth pressure—displacement curve under the cyclic loading are soil stiffness in unload and reload stages. In this subsection, first, the relationship between the soil stiffness in unloading and the earth pressure just before unloading is demonstrated. And then, degradation of the soil stiffness in reloading in relation to the infilling soil index (δ_F) that represents amount of soil that pins in the gap in unload phase is illustrated.

Figure 14 plots relationships between the soil stiffness in unloading, K_U, and the earth pressure just before unloading, σ_{hU}. The soil stiffness is taken as the slope of a linear portion of the unloading curve and the earth pressure just before unloading corresponds to that at Point A in Fig. 8. Even though the plots are scattered, the soil stiffness in unloading stages increases with the earth pressure just before unloading. This suggests that the soil stiffness in unloading stages can be modelled as a function of the earth pressure just before unloading, such as:

$$K_U = K_{U0}\left(\frac{\sigma_{hU}}{P_a}\right)^n, \qquad (2)$$

where P_a = atmospheric pressure, K_{U0} = soil stiffness in unloading when $\sigma_{hU} = P_a$ and n = material constant. This empirical equation is analogy of those on shear modulus at the small strain level (Hardin & Richart 1963, among others.) In the tests, $K_{U0} = 10$MPa and $n = 0.5$ for Toyoura sand, while $K_{U0} = 7.3$MPa and $n = 0.7$ for Edosaki sand. Here the earth pressure just before unloading is selected as a representative stress parameter. However, the soil stiffness in unloading does not have to be a function of the earth pressure just before unloading, as long as the stress dependency of the soil stiffness is considered in the modelling.

Figure 15 plots changes of soil stiffness ratio, K_R/K_U with the infilling soil index, δ_F normalised by the pile cap embedment depth, D. The soil stiffness is taken as the slope of a linear portion of the reloading curve and δ_F represents amount of closure of the gap in unload phase as shown in Fig. 8. The ratio of the soil stiffness in reload phase to that in unload phase, K_R/K_U, decreases with the infilling soil index, δ_F, and the relationships seem to fit an unique line in the tests, irrespective of the sands used:

$$\frac{K_R}{K_U} = \frac{1}{1+\left(\frac{1}{R_0}-1\right)\frac{\delta_F}{D}}, \tag{3}$$

where $R_0 = K_R/K_U$ when $\delta_F = D$. In the tests, $R_0 = 0.0133$.

Using Eqns. (2) and (3), the soil stiffness in unload and reload stages can be modelled, provided the earth pressure just before unloading (σ_{hU}) and the infilling soil index (δ_F) that represents amount of soil that pins in the gap in unload phase.

Comparisons of simple empirical model and observed earth pressure change

Using the above information, a simple empirical model that can be used for the beam on non-linear Winkler foundation type analysis is proposed. The model consists of

1. Assumption for gap opening and closing, depending on the soil type ($\delta_G = 0$ for (nearly) dry sand, while $\delta_F = 0$ for moist sand. See Fig. 8 for the definitions.),
2. Backbone curve obtained from the monotonic loading test,
3. Reference particle that is (1) not far from the pile cap and (2) free from the cyclic-loading-induced relocation process of soil adjacent to the pile cap,
4. Relationship that associates the pile cap displacement with the reference particle displacement (Eqn. (1)), and
5. Soil stiffness in unload (K_U) and reload (K_R) phases (Eqns. (2) and (3).)

When δ_F is assumed to be zero, the reload curve retraces the unload curve, thus, $K_R = K_U$.

To compare the response of the simple empirical model with the observed earth pressure change, the backbone curves are approximated by hyperbolic curve:

$$\sigma_h = \frac{K_{B0}}{1+\frac{u_R}{u_0}} u_R = f_B(u_R), \tag{4}$$

where K_{B0} = coefficient of initial subgrade reaction and $K_{B0}u_0$ = passive earth pressure. For Toyoura sand with $D/H = 2$, $K_{B0} = 3.54\times10^5$ (kN/m^3) and $u_0 = 1.19\times10^{-3}$ (m), while $K_{B0} = 3.30\times10^5$ (kN/m^3) and $u_0 = 1.64\times10^{-3}$ (m) for Edosaki sand with $D/H = 2$.

These parameters were obtained from the fittings of the function to the monotonic loading curve in range of $u_R/H = u/H < 50\%$.

The earth pressure—pile cap displacement curve is bounded by the backbone curve (the upper bound) and the lower limit of the earth pressure, i.e., the active earth pressure, σ_{hA}:

$$\sigma_{hA} \le \sigma_h \le f_B(u_R) = \frac{K_{B0}}{1 + \frac{f_R(u, \dot{\delta}_F, t)}{u_0}} f_R(u, \dot{\delta}_F, t). \quad (5)$$

When the current state point is inside the boundary in the earth pressure—pile cap displacement plane, the earth pressure—pile cap displacement relation is modelled by linear curve with the soil stiffness given by either Eqn. (2) or (3).

Figure 16 plots the observed and calculated earth pressure vs normalised pile cap horizontal displacement curve, together with the earth pressure change time histories for the Toyoura sand test for Cyclic2 with $D/H = 2$. The similar plots for the Edosaki sand test are shown in Fig. 17. In the calculation, (1) the earth pressure changes were calculated using the observed pile cap displacement time histories, and (2) the lower limit of the earth pressure, σ_{hA}, was assumed zero. As the earth pressure change in unload and reload phases are modelled by the linear earth pressure—displacement relation, the concave up and down type behaviour cannot be captured. However, the overall earth pressure responses can be modelled by the simple empirical model both in the Toyoura and Edosaki sand tests as shown in the figures.

For the Toyoura sand test, before reaching the passive state, i.e., in Phases 1 and 2, the simple empirical model can capture the earth pressure change observed in the physical model test, especially the fact that the maximum earth pressure mobilised increases with each successive loading cycle in a loading phase, as mentioned in the previous section. However, once the mobilised earth pressure reaches the passive in Phase 3, the calculated earth pressure in the following phases (in Phases 4 and 5) overestimates the observed one. This is mainly due to the overestimate of u_R in the calculation, as δ_G is assumed zero. For the Edosaki sand test, in the monotonic loading phase following the cyclic loading, as $\delta_F \neq 0$ in the physical model test, the earth pressure is underestimated at the beginning of the monotonic loading phase.

For application of model proposed

Physical model tests reveal that mobilisation of the earth pressure acting on pile caps under cyclic loading can drastically change depending on soil type and/or conditions. The tests demonstrate two completely different responses of the soil adjacent to the pile cap: When the soil adjacent to the pile cap easily causes the active failure in unload phase like the dry Toyoura sand, filling-the-gap process in unload phase dominates the earth pressure—displacement curve. On the contrary, if such active failure does not occur due to apparent cohesion when unloaded, as in the moist Edosaki sand tests, cyclic loading merely widens the apparent gap under cyclic loading and the state point in the earth pressure—displacement plane retrace the unloading curve when reloaded.

Primarily occurrence of active failure of the soil adjacent to the pile cap when unloaded has an influence on general shape of hysteresis loop. Secondarily how the apparent gap is filled with the soil during unload phase also affects the curve shape, i.e., the reloading curve shape can change depending on the in-filled sand condition; if soil lumps fills the gap, the in-filled soil may be very compressive, while it is not so compressive when the backfill sand behaves like the dry Toyoura sand in this study. Addition to these, not only existence of apparent cohesion and the other soil conditions but also ground shaking during earthquake, which is not modelled in this study, affects the occurrence of active failure of the soil adjacent to the pile cap. With the ground shaking, the active failure may occur even for the moist sand and perhaps the general shape of the hysteresis loop approaches to that observed in the dry sand tests or in-between the dry and most sands.

When seismic performance of the lateral capacity of pile foundations is assessed without considering kinematic loads induced by interaction between the foundation and surrounding ground that vibrates and/or laterally spreads during earthquake, the moist sand type curve may gives us conservative results. However, ether can be the case if the kinematic loads are considered. In practice, as it does not seem feasible to consider all the aspects mentioned above at a time, it is advisable to analyse the seismic foundation responses with both the conditions, i.e., using the dry and moist sand models, and to adopt severe result.

SUMMARY AND CONCLUSIONS

Centrifuge model tests were conducted to demonstrate the importance of considering the effect of strain history on the load—displacement characteristics of a surface soil layer in the soil—pile cap interaction. Observations in the physical model tests reveal that mobilisation of the earth pressure acting on pile caps under cyclic loading can drastically change depending on soil type and/or conditions. Tests on dry sand show that pre-peak cyclic strains in the surface soil markedly reduce the relative displacement between the soil and pile cap that is required to reach the maximum lateral earth pressure. The process of (1) the filling a gap that has formed between the pile cap and surrounding soil in unload phase and (2) the pushing the in-filled soil forward in reload phase can make larger the strain imposed to the soil distant from the cap, resulting in a smaller pile cap displacement to cause general shear failure of the soil in front of the cap. Not only the timing of the passive earth pressure mobilisation, but also the relationship between the earth pressure and pile cap displacement during cyclic loading before reaching the passive state are affected by this relocation process of soil adjacent to the pile cap. When the surface layer is moist sand with fines like real pit-run sand, these features are less pronounced: The successive cyclic loading widens the apparent gap and the formed gap hardly closes during cyclic loading. This indicates that, unlike the dry sand, to mobilise the earth pressure acting on the pile cap during cyclic loading, the pile cap displacement comparable to or greater than the maximum displacement experienced is required for the moist sand.

Based on the observations in the physical model tests, a simple empirical model that can be used for the beam on non-linear Winkler foundation type analysis is proposed. The model consists of (1) assumption for gap opening and closing, depending on the soil type, (2) backbone curve obtained from the monotonic loading test, and (3) soil stiffness in unload and reload stages. In addition to these, to associate the current state point in the earth pressure—pile cap displacement plane with the backbone curve, a parameter that represents displacement of a reference particle in backfill is introduced. Using the simple empirical model proposed, the overall earth pressure responses can be modelled both for the dry and moist sands.

References

Berrill, J. & Yasuda, S. (2002), Liquefaction and piled foundations: some issues, *J. Earthquake Eng.*, Vol.6, Special Issue 1, 1-41.

Brandenberg, S.J., Boulanger, R.W., Kutter, B.L. & Chang, D. (2007), Liquefaction-induced softening of load transfer between pile groups and laterally spreading crusts, *J. Geotechnical and Geoenvironmental Engineering*, *ASCE*, Vol.133, No.1, 91-103.

Cole, R.T. & Rollins, K.M. (2006), Passive earth pressure mobilisation during cyclic loading, *J. Geotechnical and Geoenvironmental Engineering*, *ASCE*, Vol.132, No.9, 1154-1164.

Duncan, J.M. & Mokwa, R.L. (2001), Passive earth pressures: theories and tests, *J. Geotechnical and Geoenvironmental Engineering*, *ASCE*, Vol.127, No.3, 248-257.

Fang, Y.S. Chen, T.J. & Wu, B.F. (1994), Passive earth pressure with various wall movements, *J. Geotechnical Engineering*, *ASCE*, Vol.120, No.8, 1307-1323.

Fang, Y.S., Chen, J.M. & Chen, C.Y. (1997), Earth pressures with sloping backfill, *J. Geotechnical and Geoenvironmental Engineering*, *ASCE*, Vol.123, No.3, 250-259.

Finn, W.D.L. & Fujita, N. (2005), Piles under seismic excitation and lateral spreading in liquefiable soils, *Proc Geotechnical Earthquake Engineering Satellite Conference –Performance based design in earthquake geotechnical engineering: concepts and research–*, *Osaka*, *Japan*, 207-214.

Hardin, B.O. & Richart, F.E. (1963), Elastic wave velocities in granular soils, *J. Soil Mechanics and Foundations, ASCE*, Vol.95, SM1, 1531-1537.

James, R.G. & Bransby, P.L. (1970), Experimental and theoretical investigations for a passive earth pressure problem, *Géeotechnique*, Vol.20, No.1, 17-37.

Mokwa, R.L. & Duncan J.M. (2001), Experimental evaluation of lateral-load resistance of pile caps, *J. Geotechnical and Geoenvironmental Engineering*, *ASCE*, Vol.127, No.2, 185-192.

Narain, J. Saran, S. & Nandakumaran, P. (1969), Model study of passive presure in sand, *J. Soil Mechanics and Foundations Division*, *ASCE*, Vol.95, No.4, 969-983.

Ng, C., Springman, S. & Norrish, A. (1998), Soil-structure interaction of spread-base integral bridge abutments, *Soils and Foundations*, Vol.38, No.1, 145-162.

Rollins, K.M. & Cole, R.T. (2006), Cyclic lateral load behavior of a pile cap and backfill, *J. Geotechnical and Geoenvironmental Engineering*, *ASCE*, Vol.132, No.9, 1143-1153.

Rollins, K.M. & Sparks, A. (2002), Lateral resistance of full scale pile cap with gravel backfill, *J. Geotechnical* *and Geoenvironmental Engineering*, *ASCE*, Vol.128, No.9, 711-723.

Rowe, P.W. & Peaker, K. (1965), Passive earth pressure measurements, *Géeotechnique*, Vol.15, No.1, 57-78.

Shirato, M., Koseki, J. & Fukui, J. (2006), A new nonlinear hysteretic rule for Winkler type soil--pile interaction springs that considers loading pattern dependency, *Soils and Foundations*, Vol.46, No.2, 173-188.

Takahashi, A., Sugita, H. & Tanimoto, S. (2006), Beam on Winkler foundation method for piles in laterally spreading soils, *ASCE Geotechnical Special Publication*, No.145, 230-241.

Takahashi, A., Sugita, H. & Tanimoto, S. (2007), Centrifuge model tests on abutments of river-crossing bridge on liquefiable soils, *Proc. 4th International Conference on Earthquake Geotechnical Engineering, Thessaloniki, Greece*, Paper No.1618.

Tokimatsu, K. (2003), Behavior and design of pile foundations subjected to earthquakes, *Proc., 12th Asian regional conference on soil mechanics and geotechnical engineering*, Vol.2, 1065-1096.

Table 1. Centrifuge model test conditions [Size: Double-columns]

Materials:	Dry Toyoura sand ($\rho_s = 2.66$Mg/m^3, $D_{50} = 0.18$mm, $D_R = 70$%) or Partially saturated compacted Edosaki sand ($\rho_s = 2.68$Mg/m3, $D_{50} = 0.25$mm, $F_C = 8.2$%, $w_{\mathrm{opt}} = 15$%, $w = 10$%, $\rho_t \approx 1.65$Mg/m^3, Relative compaction = 90%)
Depth of pile cap, *D*:	$D/H = 1$ or 2 (H : Pile cap height)
Loading patterns:	- Monotonic - Cyclic1 (Horizontal relative displacement between soil and pile cap gradually increases during cyclic loading.) - Cyclic2 ("Two-way" cyclic loading followed by monotonic loading)

Table 2. Peak strength parameters obtained from direct shear tests [Size: Single-column]

Material	ϕ (deg.)	c (kPa)	Range of σ'_v (kPa)
Toyoura sand	40.8	7.5	9.8—98
Interface between Toyoura sand and pile cap	33.2	11.9	49—196
Edosaki sand	37.1	9.7	9.8—98
Interface between Edosaki sand and pile cap	33.7	17.2	49—196

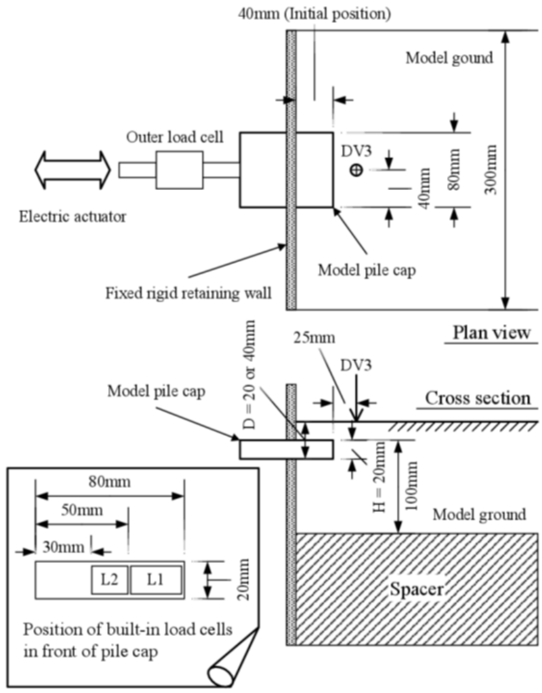

Fig. 1. Centrifuge model package. [Size: Single-column]

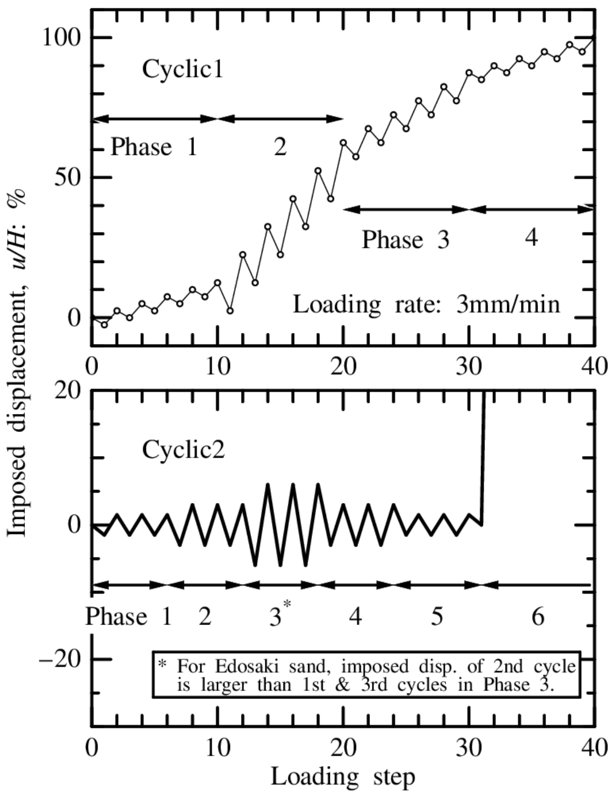

Fig. 2. Typical loading patterns. [Size: Single-column]

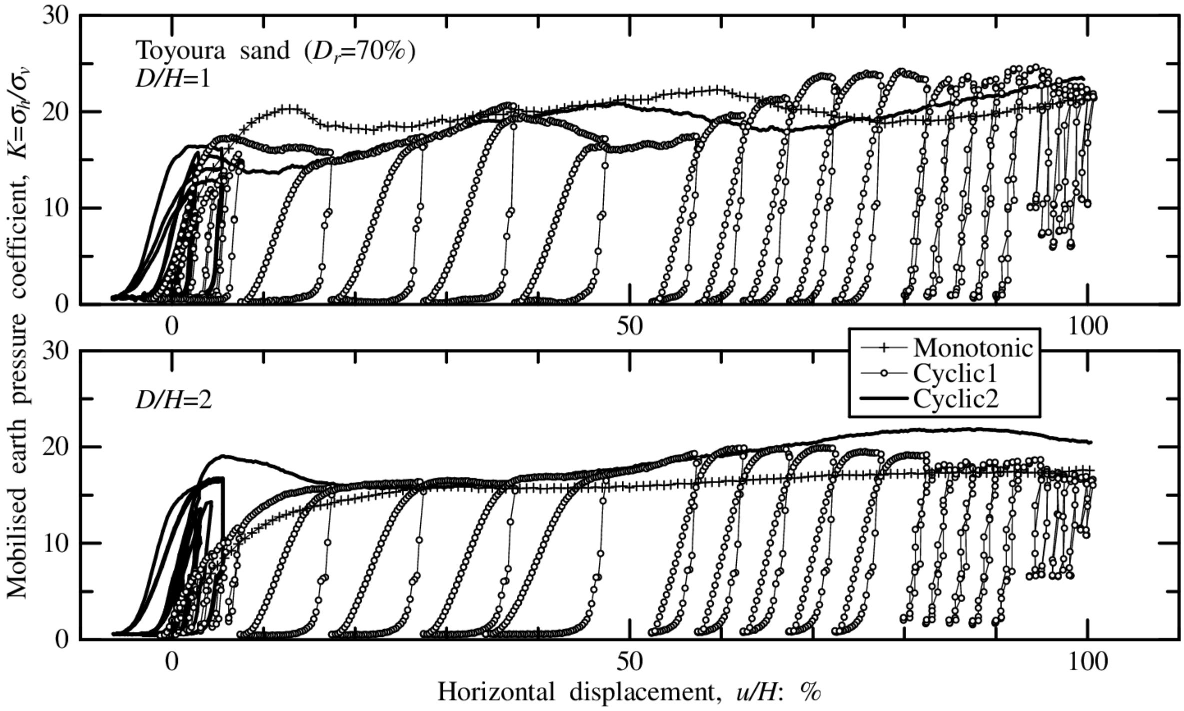

Fig. 3. Mobilised earth pressure coefficient against normalised horizontal displacement of pile cap for Toyoura sand cases. [Size: Double-columns]

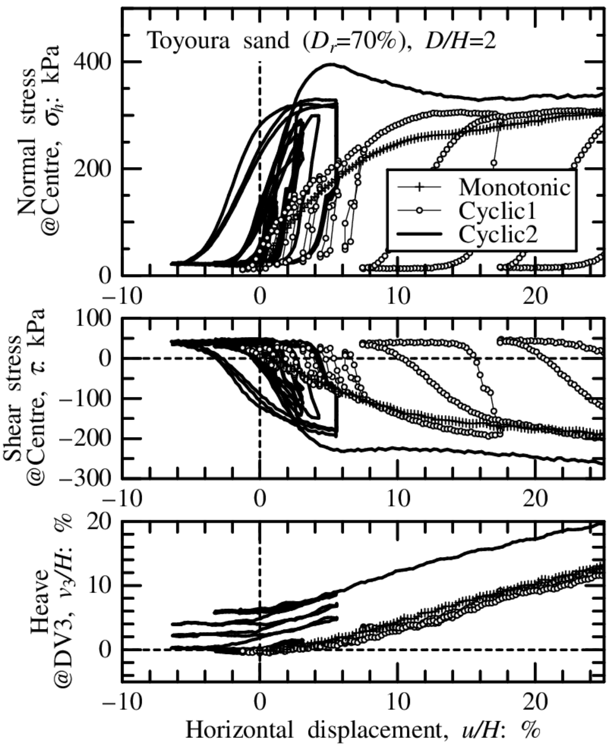

Fig. 4. Changes of normal and shear stresses acting on pile cap against normalised horizontal displacement for Toyoura sand with $D/H=2$ (measured at L2), together with changes of heave of ground surface in proximity of cap at DV3. [Size: Single-column]

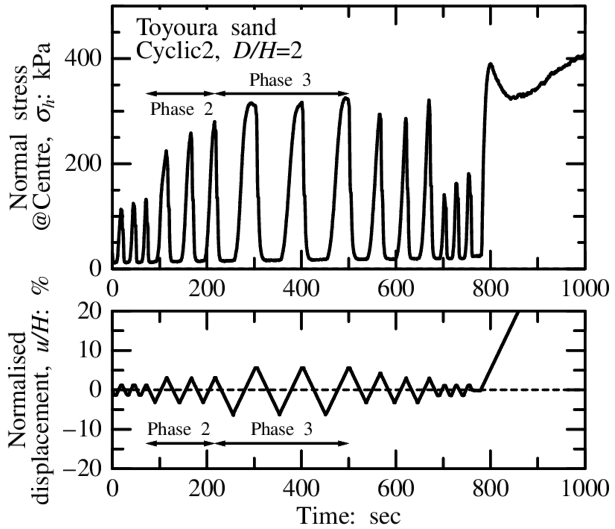

Fig. 5. Time histories of normal stress measured at L2 and normalised imposed displacement for Toyoura sand Cyclic2 with $D/H = 2$. [Size: Single-column]

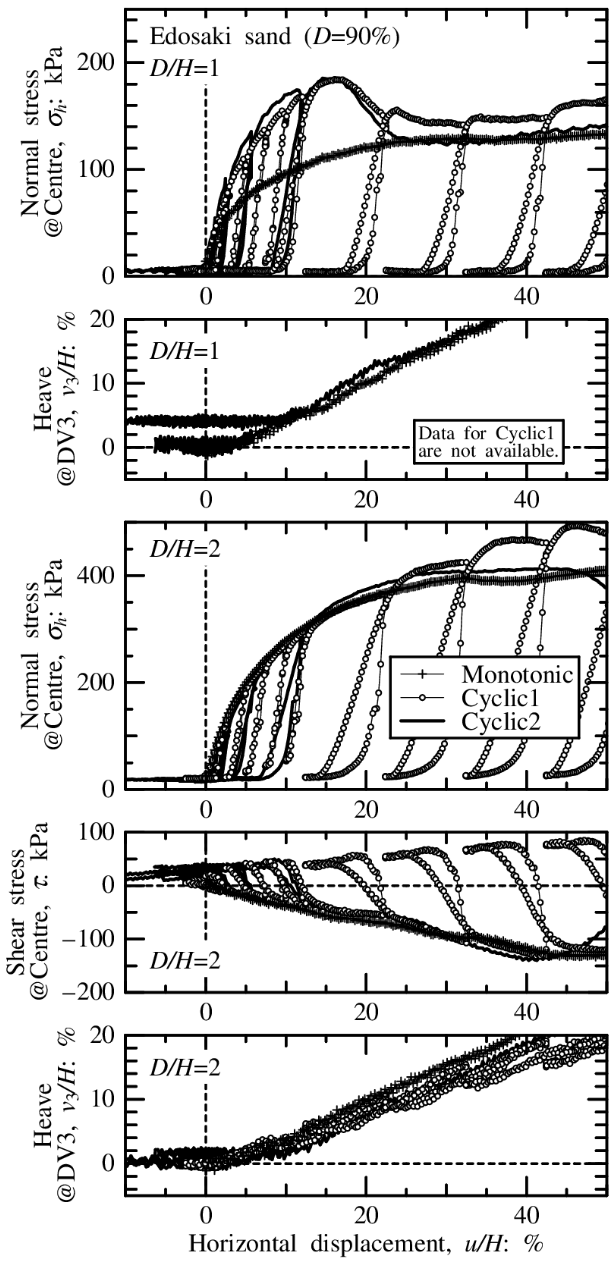

Fig. 6. Changes of normal and shear stresses acting on pile cap against normalised horizontal displacement for Edosaki sand (measured at L2), together with changes of heave of ground surface in proximity of cap at DV3. [Size: Single-column]

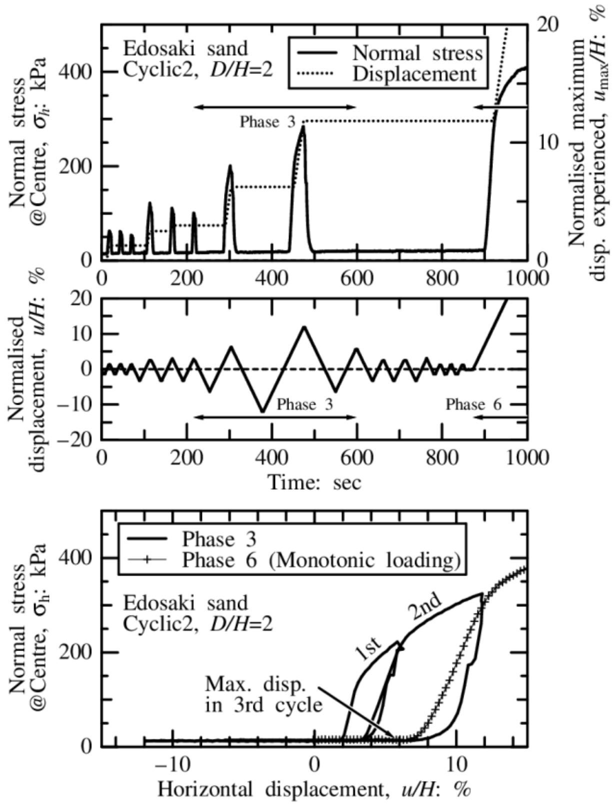

Fig. 7. Time histories of normal stress measured at L2, normalised maximum pile cap displacement experienced and normalised imposed displacement for Edosaki sand Cyclic2 with $D/H=2$, together with earth pressure vs displacement curves in Phases 3 and 6 (monotonic loading that follows cyclic loading.) [Size: Single-column]

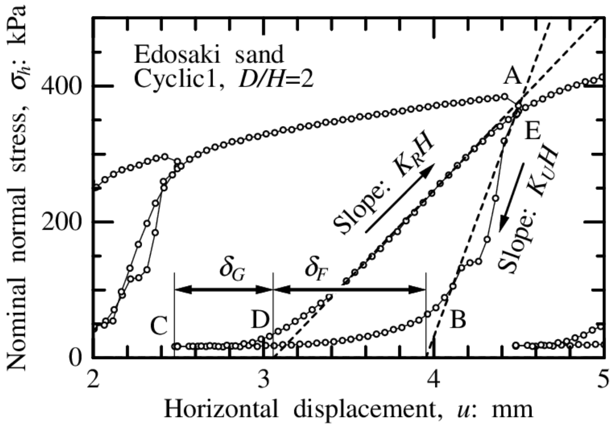

Fig. 8. Definitions of δ_G and δ_F, where $\delta_G =$ apparent gap and $\delta_F =$ infilling soil index representing amount of soil that pins in gap when unloaded. [Size: Single-column]

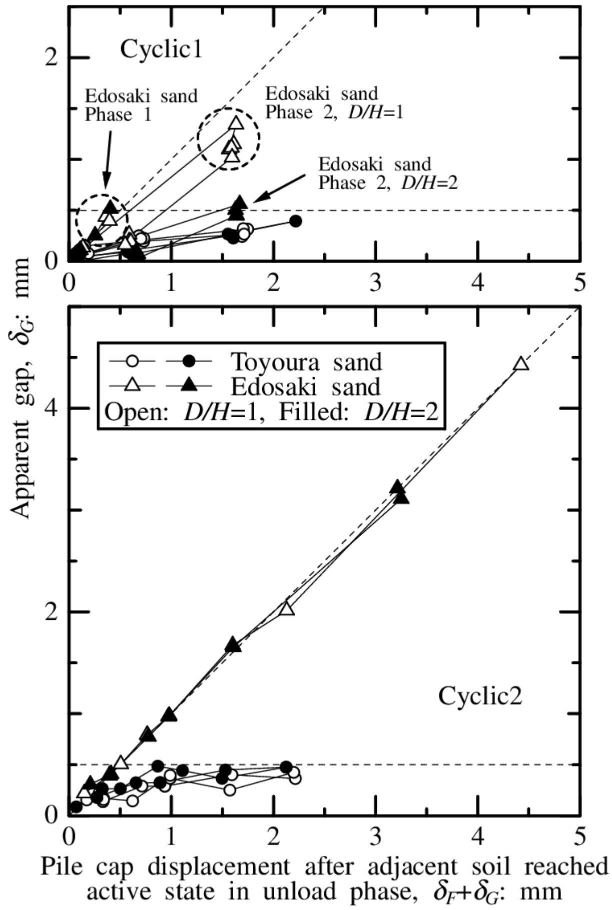

Fig. 9. Changes of apparent gap with pile cap displacement after adjacent soil reached active state in unload phase. [Size: Single-column]

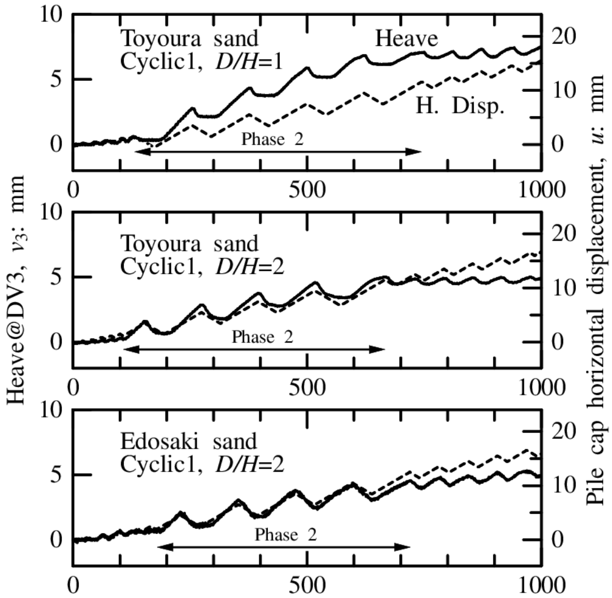

Fig. 10. Time histories of heave of ground surface in proximity of cap at DV3 and horizontal displacement. [Size: Single-column]

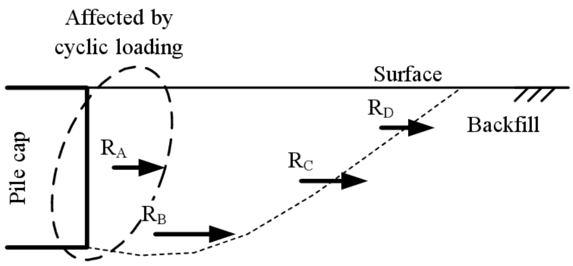

Fig. 11. Displacements required to mobilise passive earth pressure. [Size: Single-column]

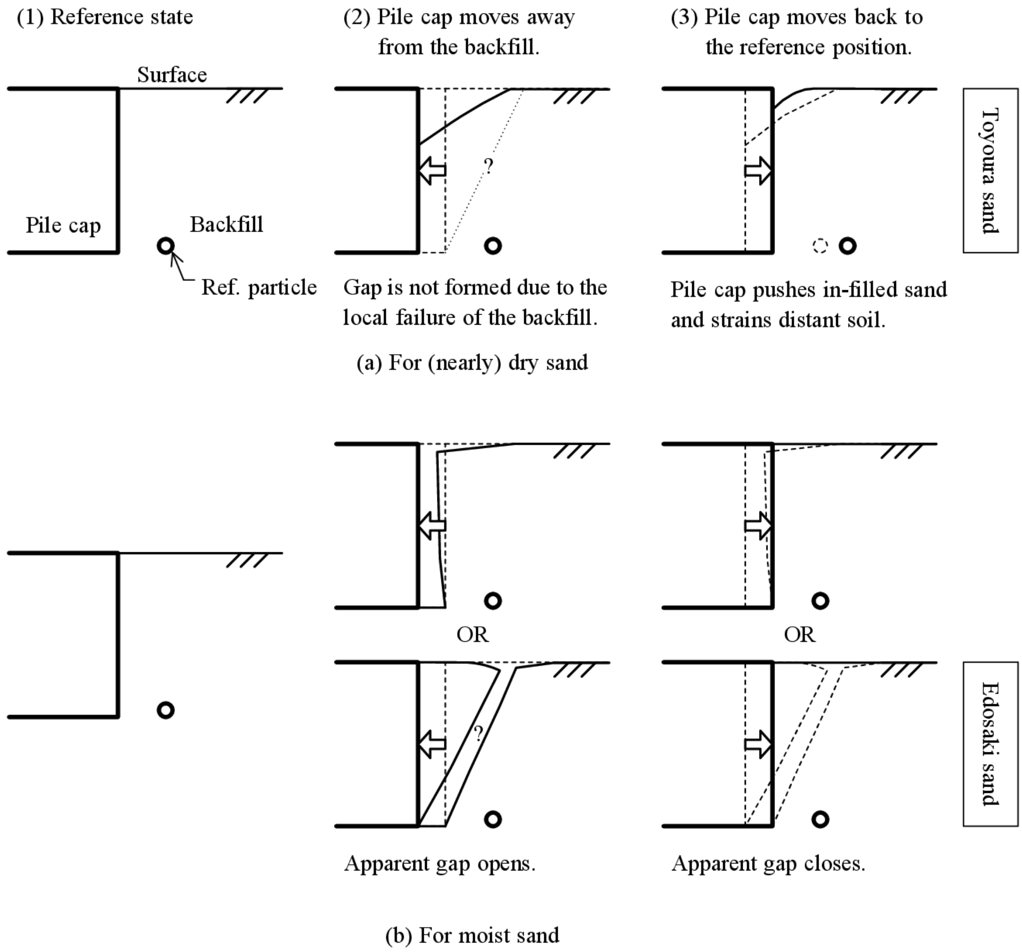

Fig. 12. Deformation of sands adjacent to pile caps in unload—reload cycle. [Size: Double-columns]

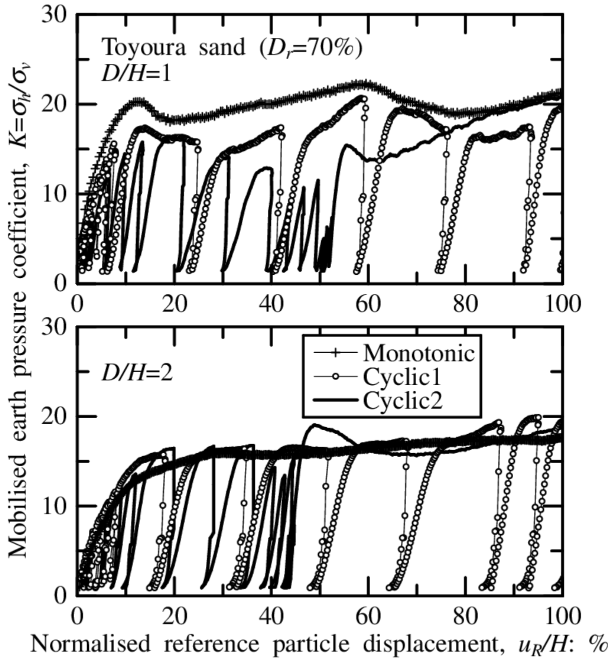

Fig. 13. Mobilised earth pressure coefficient against normalised reference particle displacement for Toyoura sand cases. [Size: Single-column]

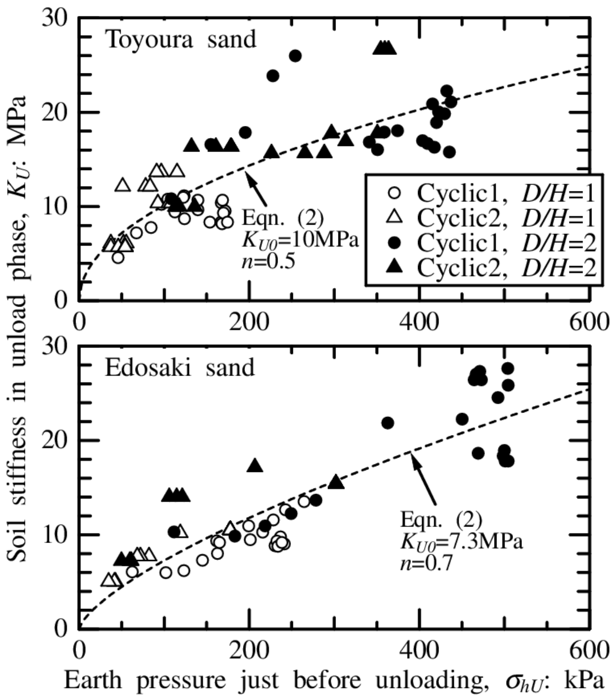

Fig. 14. Changes of soil stiffness in unload phase with earth pressure just before unloading. [Size: Single-column]

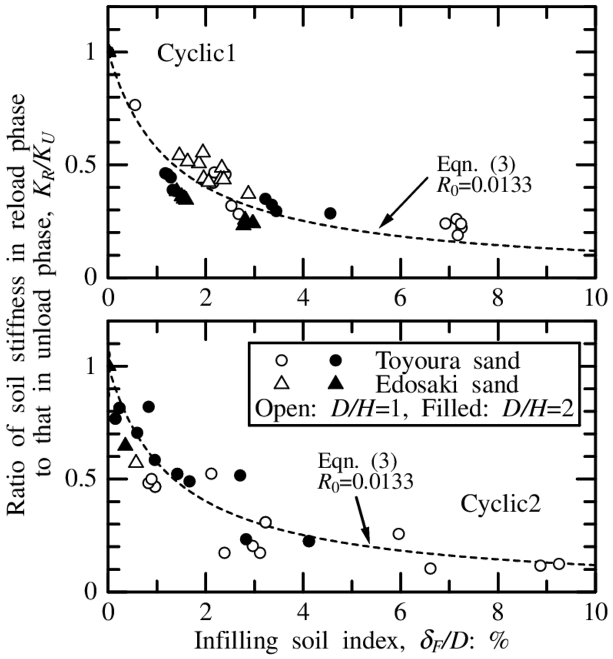

Fig. 15. Changes of soil stiffness ratio with infilling soil index, δ_F. [Size: Single-column]

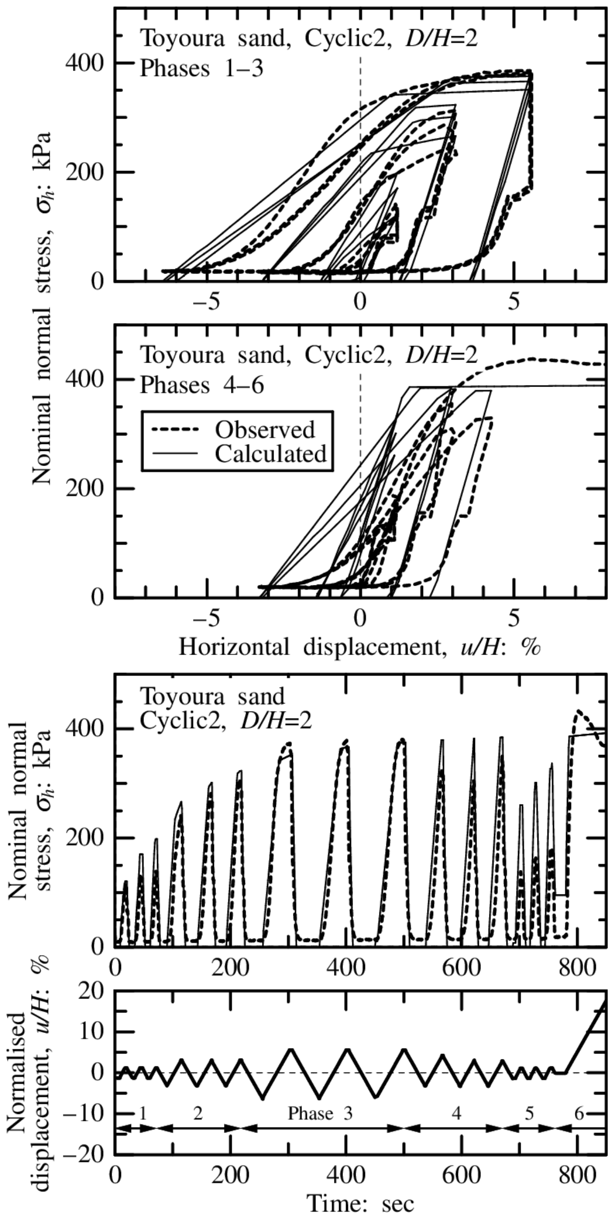

Fig. 16. Comparisons of observed and calculated earth pressure changes for Toyoura sand (Cyclic2, $D/H = 2$).

[Size: Single-column]

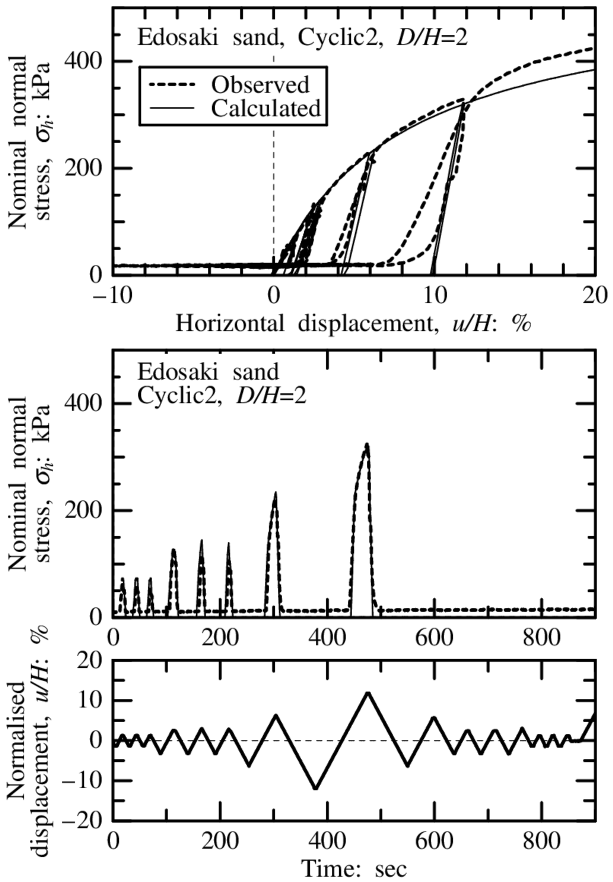

Fig. 17. Comparisons of observed and calculated earth pressure changes for Edosaki sand (Cyclic2, $D/H = 2$).

[Size: Single-column]